

# Vanadium-Catalyzed Oxidation of Terminal Olefin with Molecular Oxygen: Competing Products between Epoxide and Aldehyde

Muhamad Abdulkadir Martoprawiro<sup>a</sup>, Risma Yulistiana<sup>a</sup>, Yessi Permana<sup>a</sup> \*, Arifin<sup>b,c</sup>, Stephan Irle<sup>b,d</sup>

<sup>a</sup> Inorganic and Physical Chemistry Research Division, Institut Teknologi Bandung,

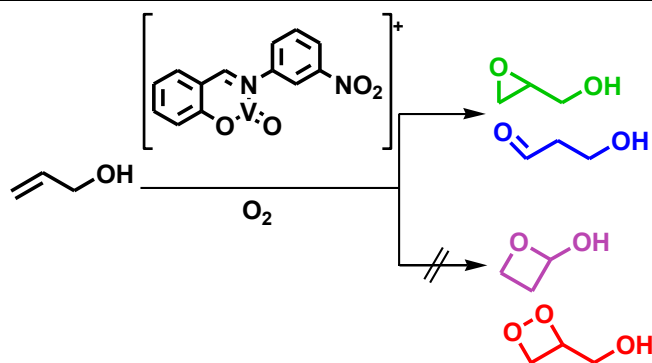
Jl. Ganesha 10, Bandung 40132, Indonesia

<sup>b</sup> Institute of Transformative bio-Molecules (ITbM), Nagoya University, Nagoya 464-8602, Japan

<sup>c</sup> JSR Corporation, Japan

<sup>d</sup> Oak Ridge National Laboratory, US

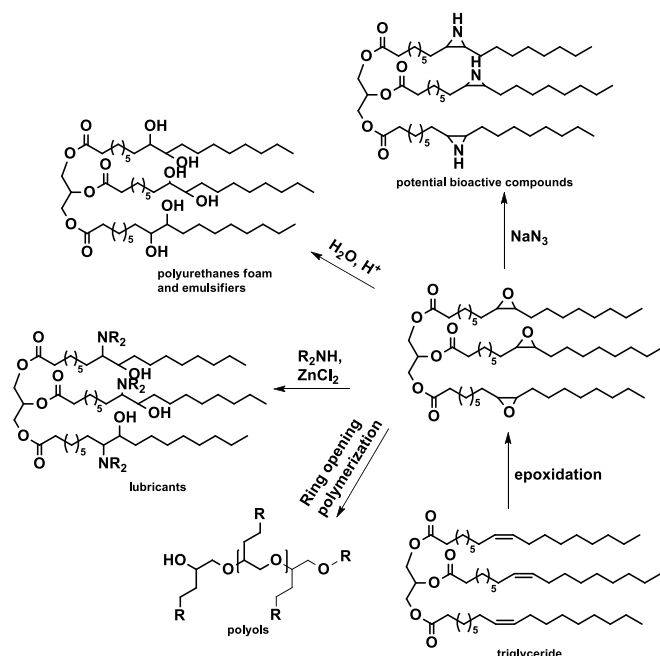
Supporting Information Placeholder



**ABSTRACT:** Oxidations of allyl alcohol and 1-hexene with vanadium(IV)oxo phenoxyimine as catalyst and  $O_2$  as oxidizing agent were discussed herein, based on *ab initio* study of their possible reaction routes using DFT with B3LYP functional and basis set of cc-pVDZ for all atoms. An uncatalyzed-activation of molecular oxygen, by which oxygen directly attacks to olefin, was both kinetically ( $\Delta G^\ddagger > 300$  kJ/mol) and thermodynamically ( $\Delta G > 300$  kJ/mol) not preferable in contrast to the catalyzed-activation of molecular oxygen by a single electron transfer (SET) ( $\Delta G = -14.36$  kJ/mol). Isomerization of  $\eta^1-O_2$  to  $\eta^2-O_2$  complex apparently underwent via a small energy barrier ( $\Delta G^\ddagger = 12.3$  kJ/mol). Product dissociation of epoxidized allyl alcohol from the complex in the last step likely to be the rate determining step as it required the highest energy ( $\Delta G = 235.27$  kJ/mol) among all steps. Interestingly, energy involved in the dissociation of 1-epoxyhexane from the complex was much smaller ( $\Delta G = 163.52$  kJ/mol) compared to that of epoxidized allyl alcohol, describing deceleration effect of a polar moiety.

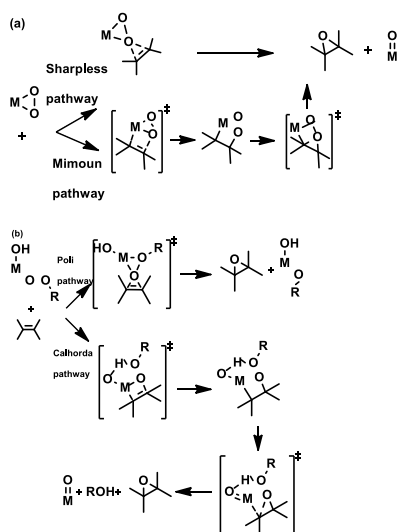
## 1. INTRODUCTION

Production of future fine chemicals are projected to deploy bioresources to alleviate the environmental risk and depletion of petroleum production. Epoxides, as versatile intermediates to produce other fine chemicals have attracted scientific interests in the last decades<sup>1</sup>. This is because epoxides have high strained-ring to undergo electrophilic or nucleophilic ring-opening reactions.



**Scheme 1.** Possible valuable chemicals such as polyurethanes and emulsifiers <sup>2,3</sup>, bioactive compounds <sup>4-6</sup>, lubricants <sup>7-9</sup>, and other biodegradable polymers <sup>10</sup> from epoxidized vegetable oil.

Derivatives of bio-epoxides, illustrated from triglycerides containing oleic moiety, are attractive compounds because they have a broad range of applications, such as polyurethanes and emulsifiers <sup>2,3</sup>, bioactive compounds <sup>4-6</sup>, lubricants <sup>7-9</sup>, and biodegradable polymers <sup>10</sup> (Scheme 1). Although epoxides were generally synthesized satisfyingly by benign, yet corrosive oxidants such as peroxides and peracids, arising environmental issue has become a major concern <sup>11</sup>. Furthermore, problems dealing with scale-up productions are still of a major challenge.

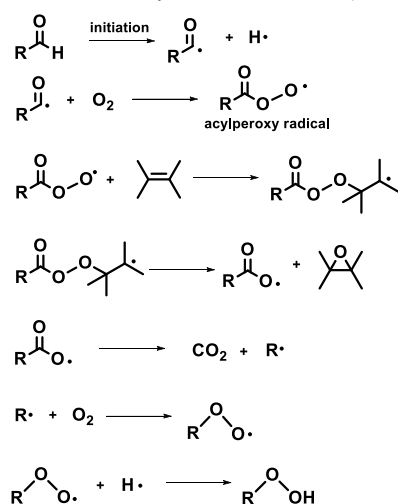


**Scheme 2.** Proposed mechanism of metal-catalyzed olefin epoxidation with organic peroxide. (a) Sharpless vs Mimoun pathway <sup>12,13</sup>. (b) Calculations conducted by Poli and Calhorda supported Sharpless and Mimoun pathways, respectively <sup>14,15</sup>.

The most well-known proposed reaction mechanism of metal-catalyzed olefin epoxidations with peroxides as oxidant was postulated by Sharpless and Mimoun, suggesting the

reaction took place from an O–O bond dissociation from a metal peroxy species (Scheme 2). According to Sharpless, olefin is not coordinated to metal, but to oxygen atom <sup>12</sup>. In contrast to Sharpless, Mimoun suggested insertion of olefin to M–O bond to generate a five-membered ring intermediate <sup>13</sup>. DFT study conducted by Calhorda and Poli supported Mimoun and Sharpless pathways, respectively <sup>14,15</sup>.

Molecular oxygen is believed to be the most promising future oxidant due to its natural abundance, green chemistry significance, and affordable price. However, it is unreactive towards uncatalyzed organic reactions <sup>11</sup> and often highly endothermic. This was proposed because its triplet state (diradical character) required another radical to react with to maintain its triplet state <sup>16</sup>. Hence, epoxidation with molecular oxygen is supposed to proceed via a mechanism that differs from epoxidation with peroxides. Excess isobutyraldehyde is commonly used as co-oxidant to activate molecular oxygen and it is proposed to generate an acyl peroxy radical as an active species from aldehyde autooxidation (Scheme 3) <sup>17</sup>.

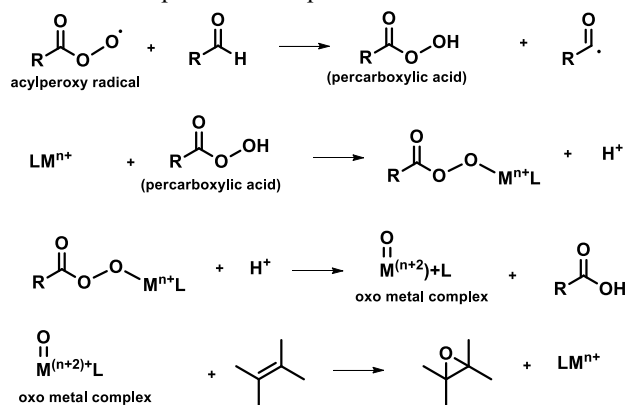


**Scheme 3.** Proposed mechanism of uncatalyzed olefin epoxidation with O<sub>2</sub> as oxidizing agent and isobutyraldehyde as co-oxidizing agent <sup>17</sup>.

Transition metal complexes have been reported to epoxidize olefins with molecular oxygen <sup>17-39</sup>. Nevertheless, isobutyraldehyde was still used as an oxygen activator, <sup>26,32,34,37</sup> particularly to enhance the selectivity towards the epoxide product. Although epoxidation of the simplest olefin, ethylene to ethylene oxide, has been industrially established with molecular oxygen and silver catalyst <sup>40</sup>, direct epoxidation of higher olefin is still challenging. Conversion of propylene to propylene oxide, for instance, was only 13% with 37% selectivity by Ag-CuCl<sub>2</sub>/BaCO<sub>3</sub> catalyst <sup>38</sup> and was 18% conversion with 44% selectivity by silica-supported molybdenum oxide catalyst <sup>20</sup>. Considerable higher selectivity to propylene oxide was achieved up to 97% by using CO/O<sub>2</sub> over Au/TiO<sub>2</sub> catalyst, yet with very low conversion (< 4%) <sup>21</sup>. The recent epoxidation of propylene achieved up to 60% selectivity and only 15% conversion in the presence of Ag–Mo–W/ZrO<sub>2</sub> catalyst <sup>41</sup>. Epoxidation of higher terminal olefins such as 1-hexene and styrene, as well as less-hindered internal olefins, such as cyclohexene, cyclooctene, and stilbenzene, solely with molecular oxygen and catalyst, also remains a major challenge. Nanoporous Au integrated with MoO<sub>3</sub> nanoparticles was reported to catalyze cyclohexene to cyclohexene oxide with conversion of only 11% and 73% selectivity <sup>39</sup>. With the help of isobutyraldehyde, activated

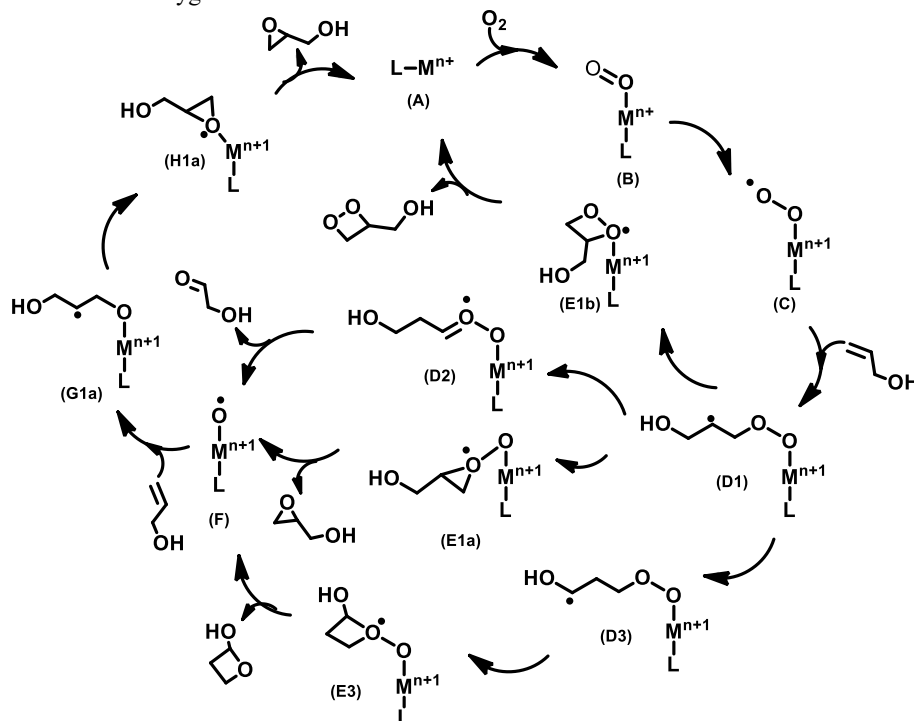
carbon-supported Pd nanoparticles was reported to catalyze cyclohexene to cyclohexene oxide with high conversion (92%) and high selectivity (96%)<sup>37</sup>. MOF-525-Mn with co-oxidizing agent of isobutyraldehyde was reported to produce styrene oxide, cyclohexene oxide, and cyclooctene oxide with 80-97% yield, as well as stilbene and 1-hexene with 75% yield<sup>34</sup>. Interestingly, oxo-vanadium(IV) tetradentate Schiff base complexes were reported to epoxidize cyclooctene and cyclohexene with high conversion (90%), although it still has a low selectivity (< 50%), when the reaction was proceeded in the absence of isobutyraldehyde<sup>42,43</sup>.

To the best of our knowledge, mechanisms involved in vanadium-catalyzed epoxidation of cyclic olefin have not been extensively studied. Therefore, epoxidations conducted at mild conditions and catalyzed by transition metal complexes to activate molecular oxygen in the absence of isobutyraldehyde would be an important development.



**Scheme 4.** Proposed mechanism of metal-catalyzed olefin epoxidation with O<sub>2</sub> as oxidizing agent and isobutyraldehyde as co-oxidizing agent<sup>26</sup>.

Epoxidations with molecular oxygen as an oxidant and



**Scheme 5.** Proposed mechanism of metal-catalyzed olefin epoxidation with O<sub>2</sub> as oxidizing agent in the absence of isobutyraldehyde.

isobutyraldehyde as a co-oxidant catalyzed by metal (M = Cr, Mn, Fe, Co, and Ni) tetraphenylporphyrin and metal (M = Mn, Fe, Co, and Cu) cyclam were previously studied through formation of a metal-oxo species (Scheme 4). The acylperoxy radical therein was likely generated through an aldehyde autooxidation<sup>26</sup>.

Oxo ligand is strongly bonded to metal center through double bond with approximately 1.6 – 1.7 Å bond length<sup>44</sup>. As a good *pi* donor ligand, oxo ligand is predicted to be unlikely to dissociate from its metal center, particularly when it is coordinated to electron-deficient metals.

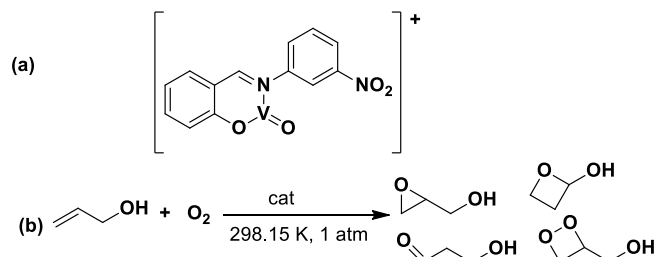
Herein, we computationally studied and proposed a mechanism of oxygen activation by a vanadium complex in the absence of isobutyraldehyde and how the activated molecular oxygen reacts with olefins, to particularly produce epoxides. We also proposed other possible products, generated from radical isomerizations. In fact, a radical mechanism was recently proposed to proceed in *cis*-cyclooctene epoxidation, catalyzed by Au cluster<sup>27</sup>.

Instead of taking an oxo ligand as an activated oxygen<sup>26</sup> (Scheme 4), we proposed that a molecular oxygen is activated through superoxide moiety generated by SET from a metal center to dioxygen ligand with  $\eta^1$ -O<sub>2</sub> geometry (Scheme 5; B to C). Geometry of complexes of  $\eta^1$ -O<sub>2</sub> is always bent at the proximal oxygen atom with decreasing  $\pi$ -interactions between the metal and the dioxygen<sup>45</sup>. Activation of <sup>18</sup>O<sub>2</sub> was previously proposed to proceed via SET in the enantioselective epoxidation of olefins catalyzed by gold complex, and this was experimentally confirmed by the existence of Au(III)/Au(I) redox cycle characterized by electrochemical and UV-Vis instrumentation<sup>33</sup>.

The mechanism (Scheme 5) is proposed initially by coordination of dioxygen ligand to the initial catalyst **A** generating dioxygen complex **B**. Activation of molecular oxygen is proposed to proceed via a peroxy radical complex generated by SET from the metal center to dioxygen ligand, and thus metal center is oxidized while dioxygen ligand is reduced in **C**. As **C** employs activated oxygen, radical oxygen is supposed to attack olefin, generating **D1**. It is worth-noting that **D1** may isomerize to **D2** and **D3**, by which each isomer may lead to different products. Carbon radical of **D1** attacks oxygen atom to generate complex employing epoxide moiety **E1a**. In addition to **E1a**, carbon radical of **D1** may also attack oxygen atom coordinated to vanadium to generate **E1b**. Dissociation of O–O bond in **E1a** generates epoxide and **F**, whereas dissociation of V–O bond in **E1b** generates dioxetane product and initial catalyst **A**.

**D2** may liberate aldehyde while **D3** may produce oxetane from **E3** moiety. If **F** employing radical is also assumed as an active catalyst, it may also attack new olefin to generate **G1**. Similar mechanism is proposed to generate **H1a**. Eventually, epoxide product is liberated and the initial catalyst **A** is regenerated to accomplish a catalytic cycle given in Scheme 5.

Several vanadium(IV) oxo-based catalyst with salen ligand were previously reported as active catalyst for epoxidation of cyclohexene and cyclooctene with 1 atm of molecular oxygen<sup>25,27,42,43</sup>. However, epoxidations of aliphatic olefin with molecular oxygen catalyzed by such vanadium complexes have not been experimentally and computationally studied. Here we studied vanadium(IV)oxo with a single bidentate phenoxyimine ligand Scheme 6(a), imitating Schiff base ligand character to epoxidize aliphatic instead of cyclic olefin with the help of Density Functional Theory (DFT). Kühn et al highlighted that a single bidentate vanadium bearing a hydroxamic acid ligand is more active in vanadium-catalyzed epoxidations of diphenyl allylic alcohol than if two bidentate ligands are attached to a vanadium center<sup>11</sup>. Allyl alcohol was used herein as an olefin model to plausibly give epoxide, aldehyde, oxetane and dioxetane products as presented in Scheme 6(b), and suggested from possible radical tautomerisms (Scheme 5). As a comparison, activation of molecular oxygen solely by olefin in the absence of catalysts and isobutyraldehyde was also computationally studied.



**Scheme 6 (a).** The catalyst model, a single bidentate phenoxyimine vanadium, mimicking a Schiff-based complex (b). Reaction model.

## 2. COMPUTATIONAL DETAILS

All calculations were performed using Gaussian09, Revision D.01 software package<sup>46</sup> and visualized with GaussView 5.0.8. Geometry optimizations, transition state (TS) identifications, frequencies and thermochemistry data were calculated using DFT with B3LYP functional and cc-pVDZ basis set for all atoms<sup>47,48</sup> in a gas phase of 298.15 K and 1.0 atm. Radical species

were calculated using unrestricted DFT to calculate open shell system. O<sub>2</sub> and radicals involved in the uncatalyzed mechanism were calculated in a triplet spin state. All species involved in the catalyzed pathways were calculated with the multiplicity of doublet, except in **TS B1B2** and **B2** which were calculated in the quartet multiplicity. Optimized structures are shown in Angstrom (Å). Hydrogen atoms are omitted for clarity when visualizing optimized structures involved in catalyzed mechanisms. When necessary, intrinsic reaction coordinate (IRC) calculation was performed to verify that the TSs were truly connected to two corresponding minima. Energy profiles were reported in kJ/mol relatively to a defined zero point.

## 3. RESULTS AND DISCUSSION

### 3.1 Mechanism of Uncatalyzed Epoxidation with Molecular Oxygen

Energy profile of allyl alcohol epoxidation in the absence of catalyst is shown in Figure 1. Yamaguchi and coworkers studied state-correlation diagrams and mechanisms for addition reactions of molecular oxygen and metal-oxo (Mn(II) and Fe(II)) species to ethylene. They found out that diradical (DR) formation, instead of a perepoxide, is the most likely mechanism to have a molecular oxygen be activated by ethylene<sup>49</sup>. Therefore, we herein referred to a diradical pathway for epoxidation of allyl alcohol in the absence of a catalyst.

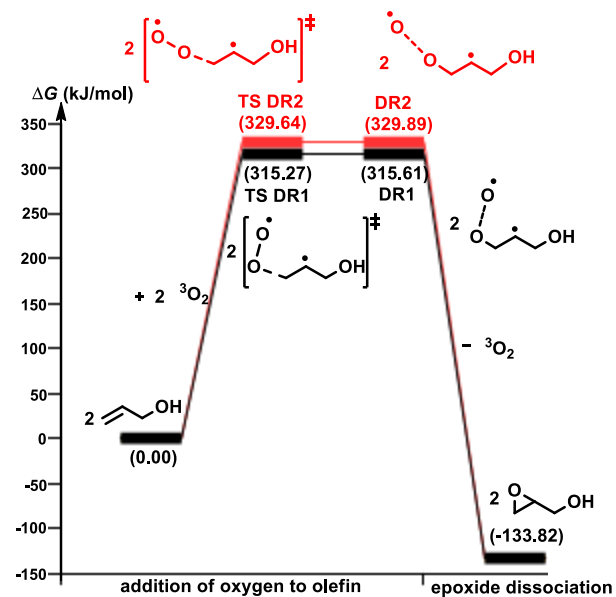


**Figure 1.** Computed free energy profiles for an uncatalyzed epoxidation of allyl alcohol with O<sub>2</sub>.

Our calculations indicate that activation of molecular oxygen directly by olefin is kinetically unlikely as it has a high activation barrier ( $\Delta G^\ddagger > 300$  kJ/mol; Figure 1). Formation of **DR1** and **DR2** from **TS DR1** and **TS DR2**, respectively are barrierless due to a radical involvement during the reaction path. Optimized geometry of intermediates and transition states involved in Figure 1 are shown in Figure 2. O<sub>2</sub> orientation to olefin relatively affects TS stability as well as its intermediates. In comparison to **TS DR2**, **TS DR1** bearing terminal oxygen closely interacts with hydroxyl proton, is considerably more stable. **TS DR1** and **TS DR2** have imaginary frequencies at  $-454.66$  and  $-523.74$  cm<sup>-1</sup>, respectively. This corresponds to stretching vibrations of oxygen atom from molecular oxygen

and carbon atom from olefin. In addition, intermediates of **DR1** and **DR2** are both high energy species ( $\Delta G > 300$  kJ/mol) and thus, formation of these intermediates are also thermodynamically unfavourable. It signifies that the relative Gibbs free energy of intermediates and transition states of diradicals was eminently close, indicating that the potential energy surface between the two coordinates is flat. Therefore, the activation of molecular oxygen directly by olefin will be kinetically and thermodynamically not preferable.

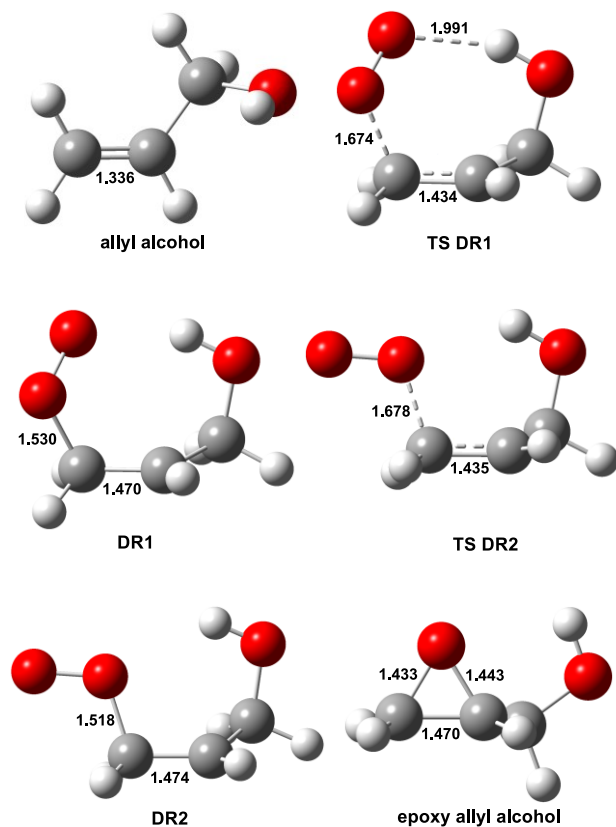


**Figure 2.** Optimized structures involved in Figure 1 (red: oxygen, grey: carbon, white: hydrogen). Bond lengths are given in Å.

### 3.2 Mechanism of Vanadium(IV) Oxo-Catalyzed Epoxidation

Free energy diagram of molecular oxygen activation and olefin attack is presented in Figure 3 and the corresponding optimized structures are shown in Figure 4. The mechanism is started by formation of dioxygen complex **B1** followed by SET to generate a peroxy radical as activated oxygen **C** (Figure 3). Formation of dioxygen complex **B1** is possible thermodynamically because it involves a bond formation between oxophilic vanadium and dioxygen ligand. In fact, dioxygen complex of vanadium(III) was previously observed by stopped flow kinetic studies<sup>50</sup>. We calculated a bond formation between dioxygen and vanadium(IV) and found that it was exothermic, with calculated energy of  $-14.36$  kJ/mol.

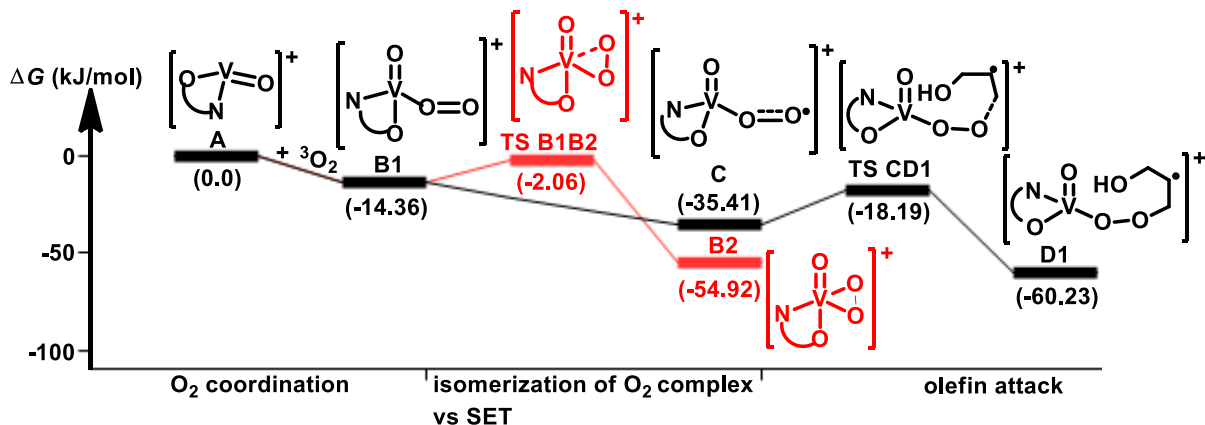


Figure 3. Computed free energy profiles for vanadium-catalyzed oxidation of allyl alcohol with  $O_2$ .

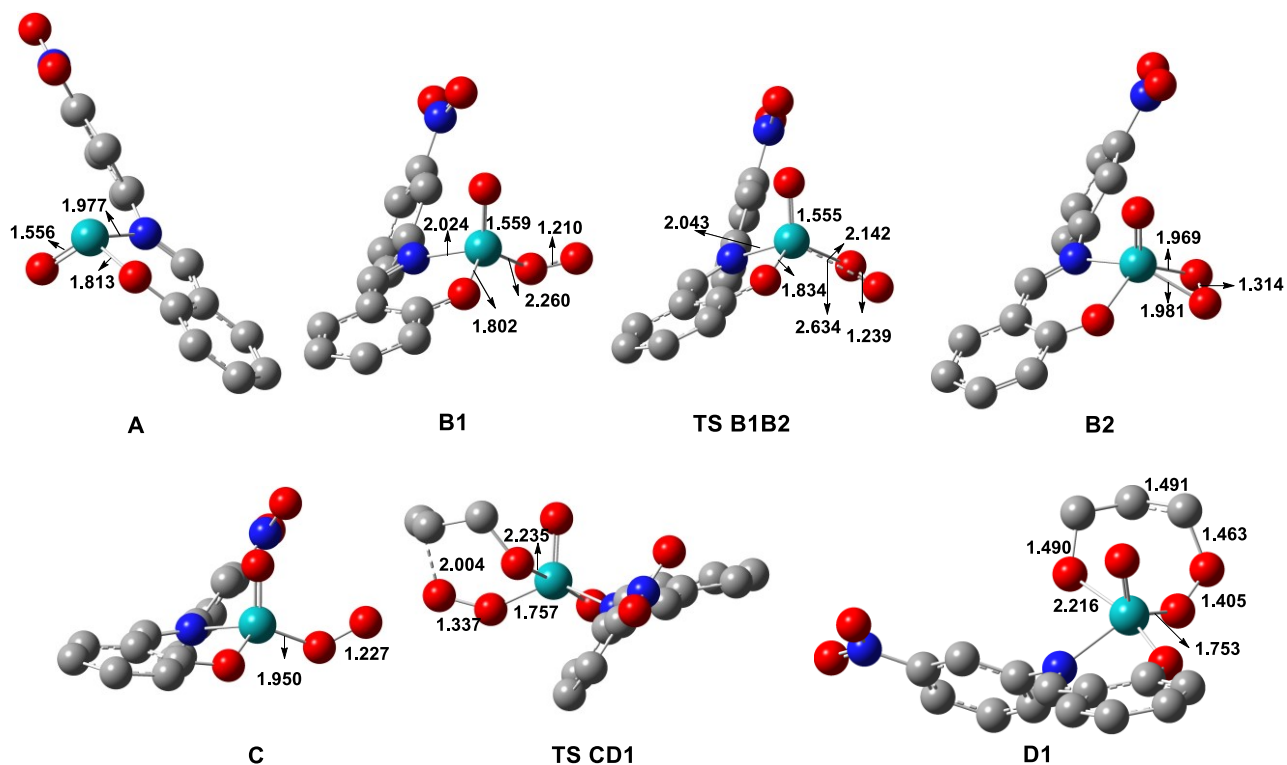


Figure 4. Optimized structures involved in Figure 3 (red: oxygen, grey: carbon, blue: nitrogen, tosca: vanadium). Bond lengths are given in Å. Hydrogen atoms are omitted for clarity.

SET was commonly observed in late transition metal complexes<sup>51–53</sup>. However, SET in early transition metal complexes were also reported<sup>54,55</sup>.

SET pathway resulted in oxidation of vanadium(IV) (**B1**) to vanadium(V), followed by a reduction of dioxygen ligand  $O_2$  to superoxide ligand  $(O_2)^{\cdot-}$  (**C**). Here, superoxide complex **C** behaves as an activated oxygen. SET of complex **B1** was thermodynamically preferable because the generated complex **C** was 21.05 kJ/mol more stable than **B1**. Both metal– $O_2$  and metal– $(O_2)^{\cdot-}$  are very distinctive in terms of O–O bond length (Figure 4; **B1** vs **C**), vibrational frequencies<sup>16</sup>, and spin states. Considering the formation of **C** from **B1** does not involve a bond-breaking and a bond-making, we assume the step proceed directly with a negligible energy barrier and thus in the absence of a transition state.

Complex **B1** may be in equilibrium with its  $\eta^2$ -counterpart

(complex **B2**). Typical isomerizations of  $\eta^1$ - $O_2$  to  $\eta^2$ - $O_2$  were previously reported in V(III) complex through a chemical equilibrium with calculated activation energy of 58.8 kJ/mol<sup>50</sup>. Here, we found a transition state between **B1** and **B2** (**TS B1B2**; Figure 4), in which  $\eta^1$ - $O_2$  isomerize to  $\eta^2$ - $O_2$  complex. **TS B1B2** has an imaginary frequency at  $-185.80\text{ cm}^{-1}$ , corresponding to a stretching vibration of terminal oxygen to vanadium to give a cyclic dioxygen, complex **B2**. Isomerization of  $\eta^1$ - $O_2$  to  $\eta^2$ - $O_2$  complex takes place via a small activation barrier ( $\Delta G^\ddagger = 12.30\text{ kJ/mol}$ ), implying a possible existence of  $\eta^2$ - $O_2$  complex. Complex  $\eta^2$ - $O_2$  **B2** is likely less reactive than  $\eta^1$ - $O_2$  **C**, because  $\pi$ -interactions between molecular oxygen and metal are greater in  $\eta^2$ - $O_2$  **B2**. As a result, molecular oxygen is less likely to be activated in  $\eta^2$ - $O_2$  **B2**. This path may be expected to be a termination step. Yet, the competing pathway (**B1** to **C**, Figure 3) may still proceed to next steps

because it proceeds with a negligible energy barrier.

As the molecular oxygen has been activated in **C**, we suggested that the addition of electron-rich olefin to oxygen will undergo via a transition state, **TS CD1** (Figure 4). Energy of 17.22 kJ/mol is necessary to conquer energy barrier to afford carbon radical **D1** and 24.82 kJ/mol is released to form a new C–O bond. **TS CD1** has an imaginary frequency at  $-352.16\text{ cm}^{-1}$ , corresponding to a stretching vibration of olefinic terminal carbon to terminal oxygen atom.

A closer inspection of **D1** also revealed the probability of a radical isomerization as a consequence of free movement of the unpaired electron within the three carbon and/or oxygen atoms. Hence it is suggested that **D2** and **D3** are the probable isomers of **D1** (Figure 5). Each radical isomer refers to a different position of carbon bonded to one hydrogen atom. Based on our calculations, **D2** is the most stable isomer, while **D1** and **D3** occupies similar energy level. Each radical isomer leads to different products. Figure 5 outlines the vis-à-vis of the

plausible pathways and Figure 6 provides the optimized structures involved in.

When **D1** does not isomerize, the unpaired electron attacks oxygen bonded to carbon atom, generating an intermediate **E1a** (Figure 5; green path). This step is thermodynamically allowed as only 5.38 kJ/mol is released because of a new bond formation of C–O to afford an epoxide ring. Although **TS D1E1a** has not been found, it can be deduced that energy barrier to afford C–O epoxide ring is relatively low as can be seen from **TS G1H1a** (Figure 7, *vide infra*), by which the activation energy of C–O epoxide formation is only 12.33 kJ/mol. Afterwards, the dissociation of epoxide product from O–O bond to give **F** undergoes via **TS E1aF** with energy barrier of only 2.97 kJ/mol (Figure 5). **TSE1aF** has an imaginary vibrational frequency at  $-519.91\text{ cm}^{-1}$ , corresponding to a stretching vibration of an epoxide dissociation (Figure 6). **F** also works as an active species to the consecutive olefin addition as it still has a coordinated oxygen with an unpaired electron.

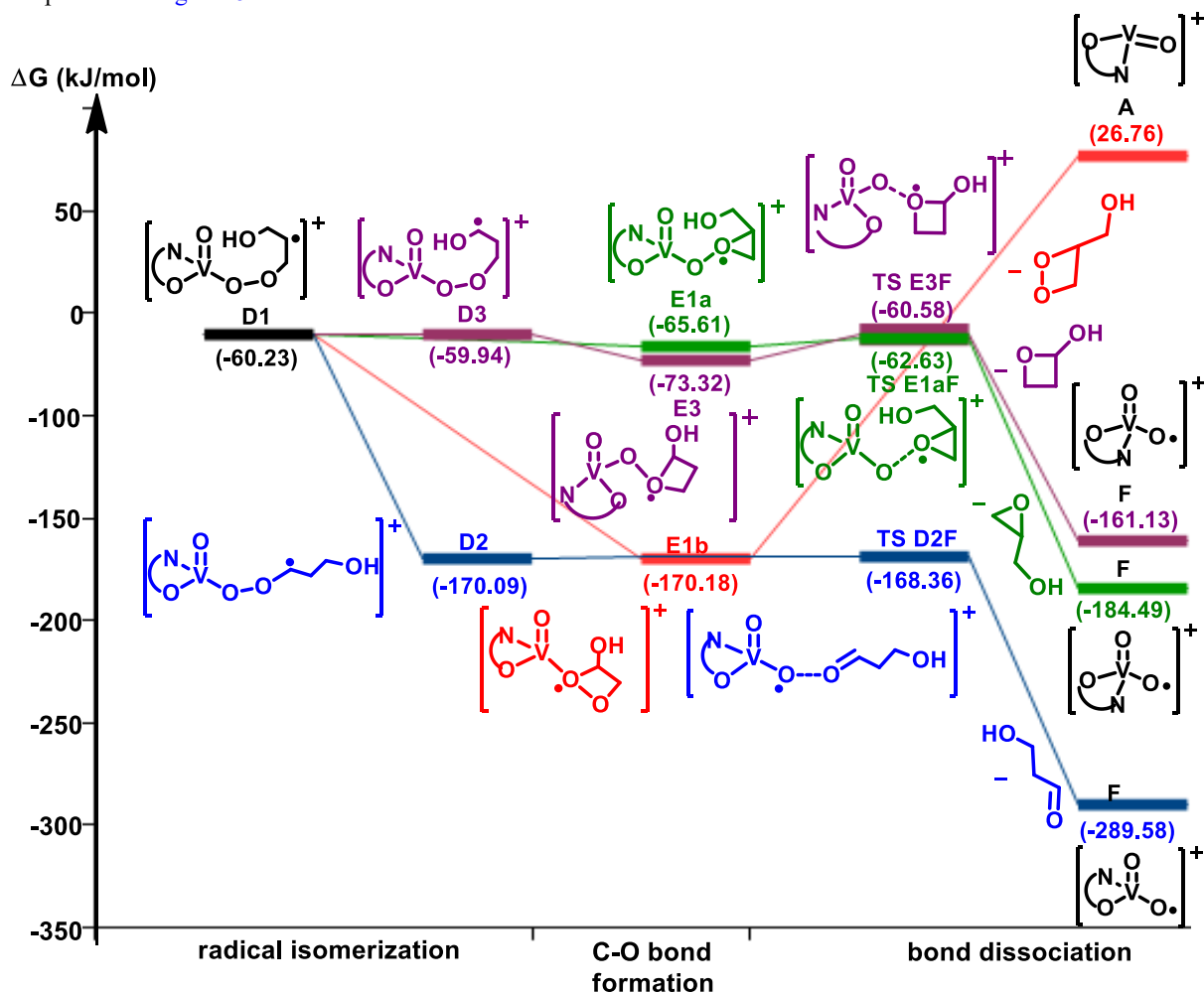


**Figure 5.** Computed free energy profiles for vanadium-catalyzed oxidation of allyl alcohol with  $\text{O}_2$  leading to dioxetane (red path), oxetane (purple path), epoxide (green path), and aldehyde (blue path).

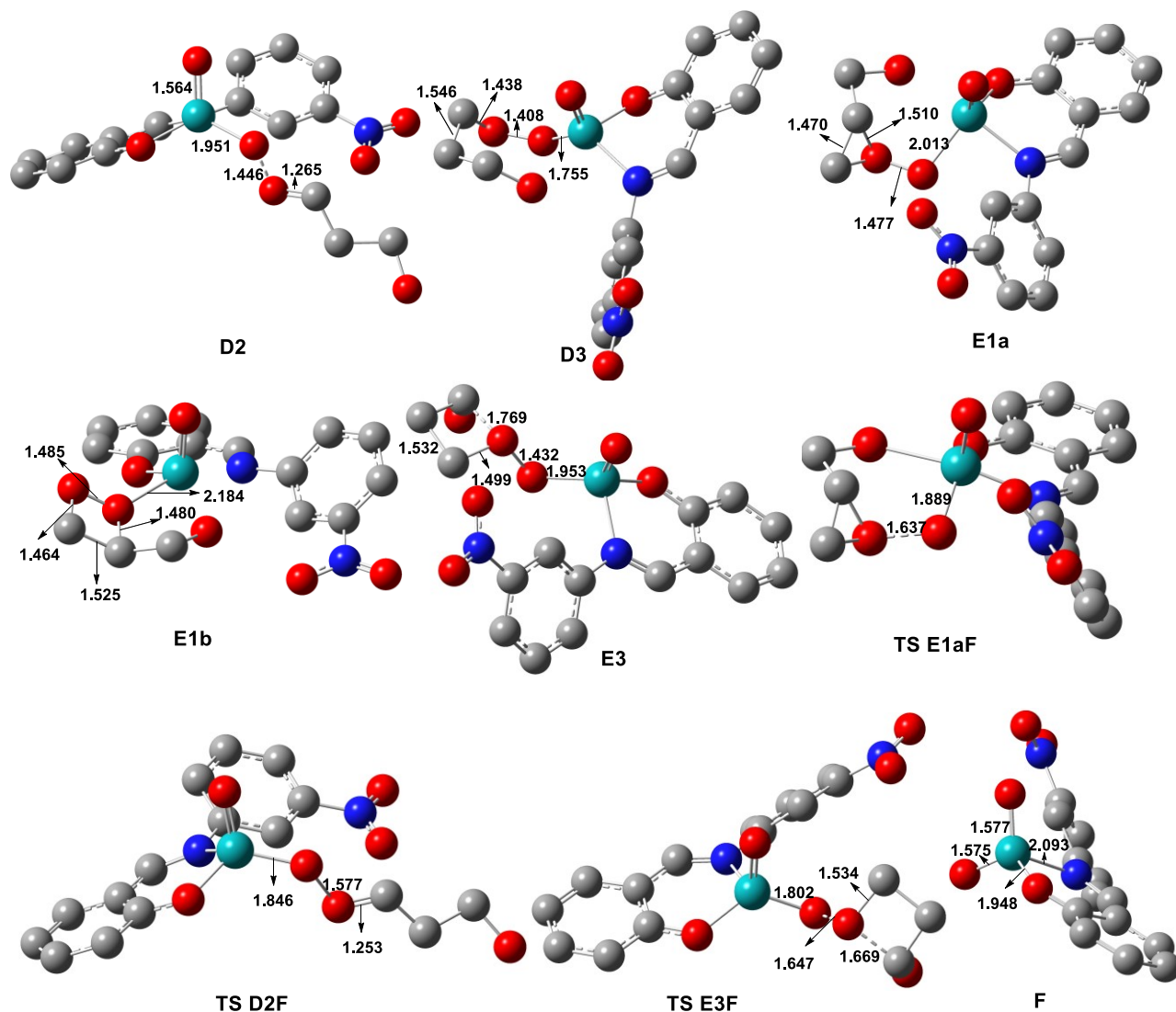


**Figure 6.** Optimized structures involved in Figure 5. Bond lengths are given in Å. Hydrogen atoms are omitted for clarity. (Red: oxygen, grey: carbon, blue: nitrogen, cyan: vanadium)

In addition to an epoxide product, **D1** may also generate a dioxetane product via a formation of an intermediate **E1b** (Figure 5; red path). Surprisingly, **E1b** is 104.57 kJ/mol more favoured over **E1a**. Nevertheless, dissociation of dioxetane product from the complex required very high energy ( $\Delta G = 196.94$  kJ/mol, Figure 5; red path). In other words, the energy barrier for dissociation of dioxetane must be greater than 196.94 kJ/mol. This might be the reason why, to the best of our knowledge, dioxetane has never been found through oxidation of olefin with molecular oxygen.

When **D1** isomerizes to **D2**, **D2** may generate an aldehyde (Figure 5; blue path). Dissociation of the aldehyde product via **TS D2F** requires low activation energy of 1.82 kJ/mol. **TS D2F** has an imaginary frequency at  $-631.88$   $\text{cm}^{-1}$ , corresponding to a stretching vibration of the aldehyde dissociation (Figure 6). Aldehydes, in fact, were found in companion with epoxides when terminal olefins were reacted with molecular oxygen using molybdenum-based complexes<sup>20,24,28</sup>, cobalt-based complex<sup>36</sup>, Ag-CuCl<sub>2</sub>/BaCO<sub>3</sub> catalyst<sup>38</sup>, and isobutyraldehyde<sup>17,26</sup>. Therein, the selectivity to styrene oxide from styrene with molybdenum-based catalyst was practically increased by increasing temperature<sup>24</sup> while the selectivity to 1-2-

epoxyhexane from 1-hexene was practically increased by decreasing temperature<sup>28</sup>. Indeed, we also found herein that the reaction pathway towards aldehyde (Figure 5, blue path) was the most favourable kinetics and thermodynamics product.

Oxetane is predicted to generate from **D3** (Figure 5; purple path). Formation of a four-membered ring intermediate **E3** is exothermic ( $\Delta G = -13.38$  kJ/mol) because a new C–O bond is formed. Dissociation of oxetane proceeds via **TS E3F** with a relatively high activation barrier ( $\Delta G^\ddagger = 12.74$  kJ/mol) compared to the transition states involved in the path of aldehyde ( $\Delta G^\ddagger = 1.82$  kJ/mol) and epoxide ( $\Delta G^\ddagger = 2.97$  kJ/mol). This might be the reason why, to the best of our knowledge, oxetane has never been found as a side product of olefin oxidation of with molecular oxygen. **TS E3F** has an imaginary frequency at  $-763.81$   $\text{cm}^{-1}$ , corresponding to a stretching vibration of four-membered ring dissociation (Figure 6).

Dissociation of dioxetane is endothermic because it involves bond-breaking of V–O to regenerate catalyst **A** (Figure 5; red path). Interestingly, dissociations of epoxide, oxetane, and aldehyde presented in Figure 5 are all exothermic. This is likely contributed from the generation of radical moiety **F**, in contrast to the pathway resulting in dioxetane that regenerates a

non-radical complex **A**. We assumed that intermediate **F** is also bearing an activated oxygen because of its unpaired electron. Because vanadium(V) has reached its highest oxidation state, this complex cannot be oxidized to vanadium(VI) to afford another oxo-complex. Yet, it remains as a vanadium(V) with a coordinated-radical oxygen (Figure 5). Contrast phenomenon was proposed previously in gold(II) superoxide to gold(III)-oxo oxidation<sup>33</sup>. Therefore, another olefin may again be oxidized by **F** through a similar path as featured in Figure 5. Nevertheless, we only calculated the epoxide formation and defined intermediate **F** as a zero point. Figure 7 points out subsequent steps for the epoxide pathway.

C–O bond formation from intermediate **F** with terminal carbon from olefin is exothermic with  $\Delta G$  stabilization of 98.56 kJ/mol (Figure 7). Although we have not found **TS FG1**, it can be deduced from **TS CD1** in Figure 5 that addition of activated oxygen to olefin proceeds via a small activation barrier ( $\Delta G^\ddagger = 24.82$  kJ/mol). This calculation reveals that three-membered ring formation via **TS G1H1a** is predicted to proceed easily via a small activation barrier ( $\Delta G^\ddagger = 11.45$  kJ/mol). **TS G1H1a** has an imaginary vibrational frequency at  $-405.85$   $\text{cm}^{-1}$ , corresponding to a stretching vibration of epoxide ring formation (Figure 9). However, a dissociation of V–O bond to regenerate the origin complex **A** and the epoxide is very endothermic ( $\Delta G = 235.07$  kJ/mol). In other words, energy barrier of epoxide dissociation from vanadium atom must be higher than 235.07 kJ/mol, implying that V–O dissociation in the last step likely to be a rate determining step (r.d.s). It can be seen that V–O bond-breaking in dioxetane dissociation (Figure 5) and epoxide dissociation (Figure 7) is very endothermic, probably due to the oxophilicity of vanadium. Although the r.d.s has an energy barrier of higher than 237.07 kJ/mol, this energy is still lower than the uncatalyzed-epoxidation of olefin with molecular oxygen ( $\Delta G^\ddagger = 315.27$  kJ/mol; Figure 1).

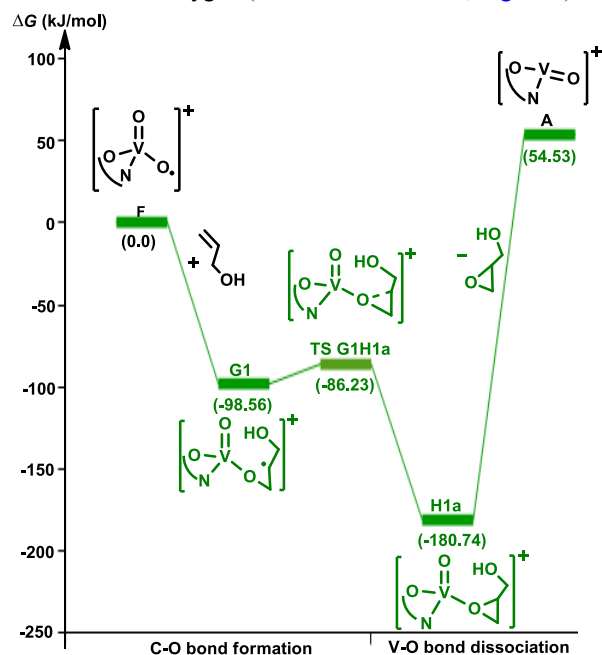


**Figure 7.** Computed free energy profiles for dissociation of epoxy allyl alcohol from catalyst.

As the oxophilicity of vanadium(IV) (complex **A**) towards hydroxyl moiety may be the cause of difficulties in the epoxide

dissociation, we compared epoxide dissociations from allyl alcohol at the last step to a non-allylic 1-hexene. We defined the complex bearing an epoxide (**H1a**) as a zero point as presented in Figure 8 (**H1a** vs **H1a'**). It reveals that dissociation of 1,2-epoxyhexane from vanadium requires noticeably lower energy than that of the epoxidized allyl alcohol (Figure 8). The dissociation of epoxidized allyl alcohol indeed requires energy of 71.75 kJ/mol higher than that of 1,2-epoxyhexane. The optimized structures involved in Figure 7 and Figure 8 are depicted in Figure 9. Epoxidations of olefins without polar moieties may be a prospective strategy in this field.

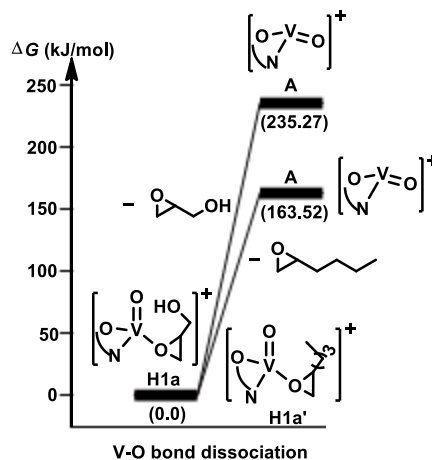


**Figure 8.** Computed free energy profiles for dissociation of epoxy allyl alcohol vs epoxyhexane from catalyst.

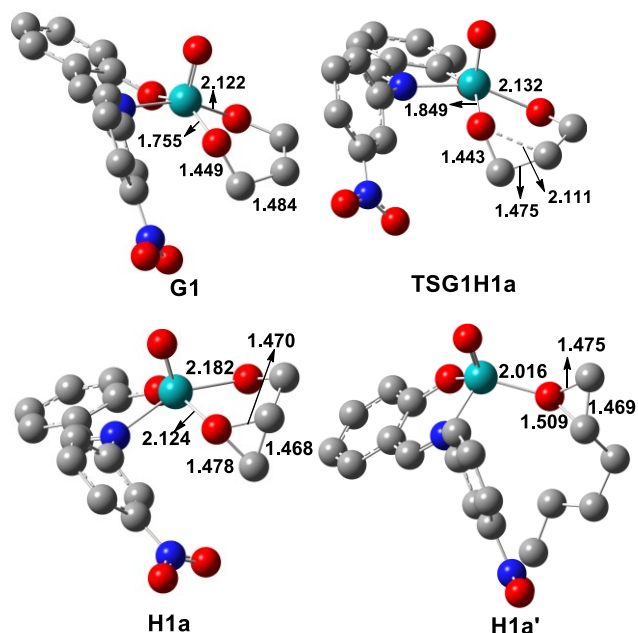


**Figure 9.** Optimized structures involved in Figure 7 and Figure 8. Hydrogen atoms are omitted for clarity (Red: oxygen, grey: carbon, blue: nitrogen, toska: vanadium)

## 4. CONCLUSION

A direct oxygen activation by olefin was kinetically and thermodynamically unfavourable ( $\Delta G^\ddagger > 300$  kJ/mol). An oxygen activation by a vanadium phenoxyimine complex via a SET mechanism was kinetically and thermodynamically favourable. Isomerization of  $\eta^1\text{-O}_2$  complex to  $\eta^2\text{-O}_2$  seemingly could undergo

via a small activation barrier. Complex  $\eta^1$ -O<sub>2</sub> radical works as an active catalyst in the olefin oxidation. Aldehyde and epoxide both may be found as products in oxidation of olefins with molecular oxygen, while oxetane and dioxetane may not. Dissociation of epoxide product in the last step might be the rate determining step. Energy involved in the dissociation of epoxides from an oxophilic complex may be lowered by eliminating a strongly coordinated functional groups. Dissociation energy of 1,2-epoxyhexane product from a vanadium phenoxyimine complex was much smaller compared to that of an epoxidized allyl alcohol. Thus, metal-catalyzed oxidations of olefins with molecular oxygen as a sole oxidant may be a prospective strategy to produce epoxides or aldehydes in a more environmentally friendly route.

## ASSOCIATED CONTENT

### Supporting Information

The Supporting Information is available free of charge on the ACS Publications website at DOI:

All computed molecule Cartesian coordinates (pdf)

## AUTHOR INFORMATION

### Corresponding Author

\* E-mail: yessi@chem.itb.ac.id

## ACKNOWLEDGMENT

This work was supported by PUPT DIKTI 2016 (No.077/SP2H/LT/DRPM/II/2016) and Indonesia Palm Oil Research Grant K-15 (No.PRJ-36/DPKS/2015) for conducting preliminary experiments on vanadium(IV) phenoxyimine-catalyzed epoxidations of olefin alcohols, alkenes, and palm oils using molecular oxygen. The funding also supported designs of theoretical study, data interpretations and manuscript preparations. We also thank Indonesia Endowment Fund (LPDP) for a master program scholarship at Chemistry Department of ITB given to RY. A acknowledges Dispatching Young Researchers Abroad Program at the Graduate School of Science, Nagoya University for a short research visit at ITB. All calculations were conducted using high performance computing (HPC) facility of Institut Teknologi Bandung (ITB) and were confirmed using computing facility of Institute of Transformative Bio-Molecules (ITbM), Nagoya University.

## REFERENCES

- Biermann, U.; Bornscheuer, U.; Meier, M. A. R.; Metzger, J. O.; Schäfer, H. J. *Angew. Chemie Int. Ed.* **2011**, *50*, 3854–3871.
- Harry-O'kuru, R. E.; Holser, R. A.; Abbott, T. P.; Weisleder, D. *Ind. Crop. Prod.* **2002**, *15*, 51–58.
- Harry-O'kuru, R. E.; Mohamed, A.; Abbott, T. P. *Ind. Crop. Prod.* **2005**, *22*, 125–133.
- Lie, M. S. F.; Jie, K.; Zheng, Y. F. **1988**, *49*, 167–178.
- Metzger, J. O.; Fürmeier, S. *European J. Org. Chem.* **1999**, *1999* (3), 661–664.
- S F, M.; Ken Jie, L.; M S K, S.-R. *Lipids* **1995**, *30* (1), 79–84.
- Biswas, A.; Adhvaryu, A.; Gordon, S. H.; Erhan, S. Z.; Willett, J. L. *J. Agric. Food Chem.* **2005**, *53*, 9485–9490.
- Harry-O'kuru, R. E.; Gordon, S. H.; Biswas, A. *J. Am. Oil Chem. Soc.* **2005**, *82* (3), 207–212.
- Pachón, L. D.; Gamez, P.; van Brussel, J. J. M.; Reedijk, J. *Tetrahedron Lett.* **2003**, *44*, 6025–6027.
- Corma, A.; Iborra, S.; Velty, A. *Chem. Rev.* **2007**, *107*, 2411–2502.
- Huber, S.; Cokoja, M.; Kühn, F. E. *J. Organomet. Chem.* **2014**, *751*, 25–32.
- Chong, A. O.; Sharpless, K. B. *J. Org. Chem.* **1977**, *42* (9), 1587–1590.
- Chaumette, P.; Mimoun, H.; Saussine, L.; Fischer, J.; Mitschler, A. *J. Organomet. Chem.* **1983**, *250*, 291–310.
- Comas-Vives, A.; Lledós, A.; Poli, R. *Chem. - A Eur. J.* **2010**, *16* (Vi), 2147–2158.
- Costa, P. J.; Calhorda, M. J.; Kühn, F. E. *Organometallics* **2010**, *29*, 303–311.
- Conry, R. R. *Encycl. Inorg. Chem. First Ed.* **2006**, 1–8.
- Wentzel, B. B.; Alsters, P. L.; Feiters, M. C.; Nolte, R. J. M. *J. Org. Chem.* **2004**, *69* (19), 3453–3464.
- Zhu, W.; Zhang, Q.; Wang, Y. *J. Phys. Chem. C* **2008**, *112*, 7731–7734.
- Zheng, X.; Zhang, Q.; Guo, Y.; Zhan, W.; Guo, Y.; Wang, Y.; Lu, G. *J. Mol. Catal. A Chem.* **2012**, *357*, 106–111.
- Song, Z.; Mimura, N.; Bravo-Suárez, J. J.; Akita, T.; Tsubota, S.; Oyama, S. T. *Appl. Catal. A Gen.* **2007**, *316* (2), 142–151.
- Sobolev, V. I.; Yu. Koltunov, K. *Appl. Catal. A, Gen.* **2014**, *476*, 197–203.
- Ségaud, N.; Anxolabéhère-Mallart, E.; Sénéchal-David, K.; Acosta-Rueda, L.; Robert, M.; Banse, F. *Chem. Sci.* **2015**, *6* (1), 639–647.
- Rao, S. N.; Munshi, K. N.; Rao, N. N.; Bhadbhade, M. M.; Suresh, E. *Polyhedron* **1999**, *18*, 2491–2497.
- Rao, S. N.; Munshi, K. N.; Rao, N. N. *J. Mol. Catal. A Chem.* **2000**, *156*, 205–211.
- Punniyamurthy, T.; Velusamy, S.; Iqbal, J. *Chem. Rev.* **2005**, *105* (6), 2329–2363.
- Nam, W.; Kim, H. J.; Kim, S. H.; Ho, R. Y. N.; Valentine, J. S. *Inorg. Chem.* **1996**, *35* (5), 1045–1049.
- Mohebbi, S.; Sarvestani, A. H. *Transit. Met. Chem.* **2006**, *31*, 749–752.
- Katkar, M. A.; Rao, S. N.; Juneja, H. D. *RSC Adv.* **2012**, *2*, 8071–8078.
- Li, X.; Fang, Y.; Zhou, X.; Ma, J.; Li, R. *Mater. Chem. Phys.* **2015**, *156*, 9–15.
- Krishnan, R.; Vancheesan, S. *J. Mol. Catal. A Chem.* **2002**, *185*, 87–95.
- Kantam, M. L.; Rao, B. P. C.; Reddy, R. S.; Sekhar, N. S.; Sreedhar, B.; Choudary, B. M. *J. Mol. Catal. A Chem.* **2007**, *272*, 1–5.
- Kameyama, H.; Narumi, F.; Hattori, T.; Kameyama, H. *J. Mol. Catal. A Chem.* **2006**, *258* (1–2), 172–177.
- Corma, A.; Domínguez, I.; Doménech, A.; Fornés, V.; Gómez-garcía, C. J.; Ródenas, T.; Sabater, M. J. *J. Catal.* **2009**, *265* (2), 238–244.
- Brown, J. W.; Nguyen, Q. T.; Otto, T.; Jarenwattananon, N. N.; Glöggler, S.; Bouchard, L.-S. *Catal. Commun.* **2015**, *59*, 50–54.
- Qian, L.; Wang, Z.; Beletskiy, E. V.; Liu, J.; dos Santos, H. J.; Li, T.; Rangel, M. do C.; Kung, M. C.; Kung, H. H.

- Nat. Commun.* **2017**, *8*, 14881–14888.
- (36) Tang, Q.; Wang, Y.; Zhang, J.; Qiao, R.; Xie, X.; Wang, Y.; Yang, Y. *Appl. Organomet. Chem.* **2016**, *30*, 435–440.
- (37) He, X.; Chen, L.; Zhou, X.; Ji, H. **2016**, *83*, 78–81.
- (38) Zhang, Q.; Chai, G.; Guo, Y.; Zhan, W.; Guo, Y.; Wang, L.; Wang, Y.; Lu, G. *J. Mol. Catal. A Chem.* **2016**, *424*, 65–76.
- (39) Dou, J.; Tao, F. (Feng). *Appl. Catal. A Gen.* **2017**, *529*, 134–142.
- (40) Rebsdat, S.; Mayer, D. *Ullmann's Encycl. Ind. Chem.* **2012**, 547–572.
- (41) Lee, E. J.; Lee, J.; Seo, Y. J.; Lee, J. W.; Ro, Y.; Yi, J.; Song, I. K. *Catal. Commun.* **2017**, *89*, 156–160.
- (42) Boghaci, D. M.; Mohebi, S. *J. Mol. Catal. A Chem.* **2002**, *179*, 41–51.
- (43) Boghaci, D. M.; Mohebi, S. *Tetrahedron* **2002**, *58*, 5357–5366.
- (44) Mayer, J. M. *Inorg. Chem.* **1988**, *27* (7), 3899–3903.
- (45) Holland, P. L. *Dalton Trans.* **2010**, *39* (23), 5415–5425.
- (46) Frisch, M. J.; Trucks, G. W.; Schlegel, H. B.; Scuseria, G. E.; Robb, M. A.; Cheeseman, J. R.; Scalmani, G.; Barone, V.; Mennucci, B.; Petersson, G. A.; Nakatsuji, H.; Caricato, M.; Li, X.; Hratchian, H. P.; Izmaylov, A. F.; Bloino, J.; Zheng, G.; Sonnenberg, J. L.; Hada, M.; Ehara, M.; Toyota, K.; Fukuda, R.; Hasegawa, J.; Ishida, M.; Nakajima, T.; Honda, Y.; Kitao, O.; Nakai, H.; Vreven, T.; Montgomery, J. A.; Jr.; Peralta, J. E.; Ogliaro, F.; Bearpark, M.; Heyd, J. J.; Brothers, E.; Kudin, K. N.; Staroverov, V. N.; Keith, T.; Kobayashi, R.; Normand, J.; Raghavachari, K.; Rendell, A.; Burant, J. C.; Iyengar, S. S.; Tomasi, J.; Cossi, M.; Rega, N.; Millam, J. M.; Klene, M.; Knox, J. E.; Cross, J. B.; Bakken, V.; Adamo, C.; Jaramillo, J.; Gomperts, R.; Stratmann, R. E.; Yazyev, O.; Austin, A. J.; Cammi, R.; Pomelli, C.; Ochterski, J. W.; Martin, R. L.; Morokuma, K.; Zakrzewski, V. G.; Voth, G. A.; Salvador, P.; Dannenberg, J. J.; Dapprich, S.; Daniels, A. D.; Farkas, O.; Foresman, J. B.; Ortiz, J. V.; Cioslowski, J.; Fox, D. J. *Gaussian, Inc., Wallingford CT* **2013**.
- (47) Becke, A. D. *J. Chem. Phys.* **1993**, *98* (7), 5648–5652.
- (48) Lee, C.; Yang, W.; Parr, R. G. *Phys. Rev. B* **1988**, *37* (2), 785–789.
- (49) Yamaguchi, K.; Yamanaka, S.; Shimada, J.; Isobe, H.; Saito, T.; Shoji, M.; Kitagawa, Y.; Okumura, M. *Int. J. Quantum Chem.* **2009**, *109*, 3745–3766.
- (50) Cozzolino, A. F.; Tofan, D.; Cummins, C. C.; Temprado, M.; Palluccio, T. D.; Rybak-Akimova, E. V.; Majumdar, S.; Cai, X.; Captain, B.; Hoff, C. D. *J. Am. Chem. Soc.* **2012**, *134* (44), 18249–18252.
- (51) Hu, X.; Li, J.; Li, H.; Zhang, Z. *J. Polym. Sci.* **2013**, *51*, 4378–4388.
- (52) Chen, K.; Zhu, Z.; Liu, J.; Tang, X.-Y.; Shi, M. *Chem. Commun.* **2015**, *52*, 350–353.
- (53) Gade, L. H. *Angew. Chemie Int. Ed.* **2000**, *39*, 2658–2678.
- (54) Potember, R. S.; Poehler, T. O.; Rappa, A.; Cowan, D. O.; Bloch, A. N. *J. Am. Chem. Soc.* **1980**, *102* (10), 3660–3662.
- (55) Williams, G. M.; Schwartz, J. *J. Am. Chem. Soc.* **1982**, *104* (1), 1122–1124.

## Table of Content

